

# Composite hollow fiber membranes for organic solvent-based liquid–liquid extraction

T. He, L.A.M. Versteeg, M.H.V. Mulder, M. Wessling\*

*Faculty of Chemical Technology, University of Twente, Membrane Technology Group, P.O. Box 217, 7500 AE Enschede, The Netherlands*

Received 14 May 2003; received in revised form 20 October 2003; accepted 1 December 2003

## Abstract

Instability issues of liquid membranes extraction significantly limit its wide application in industry. We report research on the application of a new composite hollow fiber membrane to stabilizing liquid membrane extraction. These type of composite membranes have either a polysulfone (PSf) ultrafiltration or an Accurel polypropylene microfiltration membrane as support and sulphonated poly(ether ether ketone) (SPEEK) as a coating layer. Applied as supported liquid membrane, the composite membranes showed significant improvement in stability compared to uncoated membranes. Applied in a membrane contactor, stable operation for more than 2.5 months was realized. A resistance model was developed to estimate the copper flux of the membrane contactor. The applicability of the model was proven for both the polysulfone and the polypropylene-based contactor systems. We further present the concept of encapsulated composite hollow fiber membranes with SPEEK layers encasing the extraction liquid into a hydrophobic support membrane.

© 2004 Elsevier B.V. All rights reserved.

*Keywords:* Liquid–liquid extraction; Composite membranes; Membrane contactor; Ion exchange stabilization layer

## 1. Introduction

Liquid membrane extraction is an efficient technique for the extraction of heavy metal ions from industrial effluents with the characteristics of high ion flux and high selectivity. However, the disadvantages of liquid membrane extraction, i.e. flux decline and selectivity loss, have been impeding the large scale and wide spread application in industry. In particular, supported liquid membrane extraction (SLM) suffers from instability. It is, in fact, the loss or deterioration of the organic liquid phase, which causes the instability, and it may be ascribed to several plausible mechanisms, such as solubilization, emulsion formation and osmotic pressure difference [1].

To improve the membrane stability, several solutions have been proposed in literature. The first concept was to increase the viscosity of the organic phase by stiffening the aqueous–organic interface and prevent gradual loss of organic phase [2–4]. However, the higher viscosity of organic phase causes a significant increase of the diffusional resistance. Applying a thin dense coating layer of polyvinyl chlo-

ride (PVC) on top of the support membrane between the organic and aqueous phases represents another means to stabilize the interface [5–8]. Nonetheless, the loss of organic phase continued since the hydrophobic polymer PVC could not prevent the direct contact between the two phases. Interfacial polymerization (IP) is a third technique used in SLM stabilization. In this approach, a hydrophilic polyamide layer was formed using multifunctional amines and acid chlorides as monomers [8–11]. Generally, the IP layer is permeable to mono-valent ions, but not to multi-valent ions [10]. Hence they are considered to be unsuitable for the removal of multi-valent heavy metal ions. Plasma polymerization [12] was reported to form an ultra thin skin layer as a stabilization layer, but loss of organic solvent still occurred. The increase of the overall mass transport resistance in the extra layer applied in the SLM is one of the crucial problems. Lack of a long time chemical stability of the extra layer, for example, the interfacial polymerized layer towards acid or base, is another technical obstacle. Thus, a more permeable and more chemically resistant material is required.

Instead of fabricating a complicated composite membrane, researchers attempted to manipulate the support membrane structure to achieve a stable system. A dual-skinned asymmetric microporous membrane [18], marketed as Microza™ from Pall Corporation, is anticipated to be one of

\* Corresponding author. Tel.: +31-53-489-4675; fax: +31-53-489-4611.

E-mail address: [m.wessling@ct.utwente.nl](mailto:m.wessling@ct.utwente.nl) (M. Wessling).

them. The other example is an asymmetric wettable porous membrane [19]. The membrane has a hydrophilic side and hydrophobic side, between which pores pass through in order to provide the transport. In this way, the interface between the feed solution and the extractant is substantially immobilized at the porous membrane. The advantage of this membrane configuration is that the loss of organic liquid phase due to emulsion formation is significantly decreased, theoretically giving better stability. Recently, Ho and co-workers [20–22] published a new development in the stabilization technique: the particular characteristic of this new process is a dispersion of the organic liquid phase in the strip phase, in which the loss of organic liquid phase from the aqueous phase(s) can be continuously compensated. Although the authors reported improved stability in the metal ion removal, the loss of organic phase still exists in the system and can not be considered to the final solution to instability of SLM.

Ion exchange materials were introduced to stabilize liquid membrane extraction around ten years ago and showed less transport resistance [13–16]. The work of Kedem and Bromberg [13] demonstrated promising results for the application of cation exchange membranes in liquid membrane extraction. Wijers et al. [17] recently present sandwiched flat sheet membrane, comprising thin SPEEK layers and a hydrophobic SLM in between. This membrane configuration however invokes a tremendous problem in membrane preparation scale-up, reproducibility due to bad adhesion of hydrophilic SPEEK stabilization layer to the hydrophobic PP support membrane as well as uncontrollable stress development in the composite during drying of the coating. We aim to overcome the problems of prior approaches and to prepare composite hollow fiber membranes with ion exchange stabilization layer. In particular, uncontrollable membrane undulation can be avoided by using hollow fiber since the coating stress equalizes well over the fiber circumference.

Composite hollow fibers normally carry only one hydrophilic coating preventing the loss of organic phase at one side: the membrane still has the other unprotected interface between aqueous solution and organic liquid membrane. Thus, it is the challenge to prepare a membrane, which does not suffer from the loss of organic phase, either as a fully encapsulated composite membrane, or as a membrane contactor such that complexation and de-complexation occur in two different membrane modules.

Encapsulated composite membrane was first explored by Wijers et al. using sulphonated polyetheretherketone (SPEEK) [17] and then Wang et al. using polyamide coating [11]. In this type of membrane, two stabilization layers were basically laminated onto both sides of the SLM. Layer delamination is critical due to insufficient adhesion and it constitutes a major preparation challenge. A process configuration based on stabilized configuration.

Membrane contactors is the other possible approach to overcome the problems of liquid membrane extraction. It is supposed to overcome many disadvantages of the conven-

tional extraction process such as dispersion and coalescence, emulsification, insufficient density difference between organic and aqueous phases, difficulty in scale-up [23–25]. Based on the hydrodynamics of the organic phase, two types of membrane contactor can be distinguished: (a) liquid membrane in which the organic phase is stagnant [26–29] and (b) a flowing liquid membrane in which the organic phase circulates [30–34]. A stagnant type has a mass transfer resistance approaching infinity because the organic liquid layer is thick and stationary [32]. We investigate the flowing type of membrane contactor with the new aspect of using composite membranes carrying a cation exchange layer.

We report details on the preparation of composite hollow fiber membranes and their application in SLM and membrane contactor mode. An ion exchange coating layer composed of SPEEK was selected as a model polymer for this purpose. Commercial PP Accurel hollow fiber, and tailor-made PSf membranes are used. The new concept of an encapsulated composite membrane is explored as well. Finally, a resistance model describing ion transport in membrane contactor is presented enabling a simple algorithm for membrane and process optimization. Hence, this paper describes an integrated approach to stabilize liquid membrane extraction with research activities ranging from material science, to mass transport characterization and process engineering.

## 2. Experimental

### 2.1. Materials

Poly(ether ether ketone) powder (450PF, Victrex, Mw 102,000 Da., specific density  $1.34 \text{ kg l}^{-1}$ ) was purchased from ICI. Two different support membranes were used in this experiment: a tailor-made porous polysulfone ultrafiltration hollow fiber prepared and Accurel Q3/2 and Q6/2 PP microfiltration hollow fibers provided by Membrana, Germany (formerly AKZO Nobel, Membrana). Some of their characteristic properties are listed in Table 1 at the end of the paper.

*N,N*-Methylpyrrolidone (NMP), methanol, ethanol and acetone were purchased from Merck. Copper sulfate pentahydrate,  $\text{CuSO}_4 \cdot 5\text{H}_2\text{O}$  (cryst. extra pure) and concentrated sulfuric acid (96–98%, extra pure) were purchased from Merck as well. Dodecane (with a purity of 99%) was obtained from Janssen Chimica. Henkel KgaA, Germany, supplied the extraction liquid for copper transport, LIX84-I. Ultrapure water was prepared by a MilliQ system (Millipore Corp.).

### 2.2. Preparation of SPEEK and composite membranes

Sulphonated PEEK was prepared according the procedure described in literature [17]. Sulphonation times were systematically varied between 48 and 140 h at a reaction temperature of  $T = 20^\circ\text{C}$ . SPEEK prepared for 140 h gave the highest ion exchange capacity of  $2.79 \text{ (meq g}^{-1}\text{)}$  and could be dissolved easily in almost any solvent but water.

Methanol was used a solvent: polymer solutions of 5 or 10 wt.% was filtered with a 15  $\mu\text{m}$  metal filter and de-aerated before dip-coating. The dip-coating process was carried out using a specifically designed funnel having a neck diameter being almost equal to the outside diameter of the fibers. The funnel was filled with the coating solution, with the support fiber already present in the funnel. Hence, a composite hollow fiber with an outside coating was prepared. The composite membranes were stored in an oven of 80 °C for 12 h to evaporate all solvent.

To prepare an encapsulated hollow fiber membrane, a three-step procedure was applied with succeeding coating, support impregnation and coating steps. Hence, a single-layer composite fiber—prepared as described above—was at first impregnated with the organic phase, followed by an evaporation step by flushing gaseous nitrogen for 10 s to drain out excessive amount of organic liquid off the inner surface of the hollow fiber. Finally, a SPEEK solution of 10 wt.% was introduced into the fiber bore for two times with an evaporation procedure for 30 s in between using gaseous nitrogen. After the last preparation step, the fiber was dried with nitrogen gas for 12 h before use.

To characterize the integrity of the composite membranes, composite membranes experienced the following protocol: two coated fibers with an effective length of 15 cm were first closed with hot-melt at one end; then fibers were introduced in a nylon tube (outside diameter 8 mm) and fixed with hot-melt before cut open. Nitrogen at 0.4 bar gauge was applied at the open side and the gas permeation was measured by a soap bubble flow meter. Zero permeation was defined as no observable bubble shift in a 1 ml capillary (length of 30 cm) for 5 min.

### 2.3. Copper permeation

The copper permeation procedure is similar to the one described in [17], except hollow fiber modules were used. The membrane module consisted of one (composite) hollow fiber with an effective length of 20 cm. LIX84-I diluted in dodecane to 20 vol.% was used as organic phase. A 0.025 M  $\text{CuSO}_4$  solution was used as the feed and a 2 M  $\text{H}_2\text{SO}_4$  solution as the strip. The concentrations were optimized values to give the high flux in a supported liquid membrane mode. The volume of both feed and strip was 200 ml. Unless stated otherwise, the aqueous phases circulated along the fiber with the strip solution at the shell side and the feed at the bore side. The flow velocities at the shell and bore side were 1.86 and 0.094  $\text{m s}^{-1}$ , respectively. To follow the concentration variation in the feed and strip, seven samples in 7 or 8 h interval were taken and analyzed by atomic absorption spectrometry (Spectra 10, Varian.). The copper flux was calculated from the slope of the copper concentration versus time.

For lab-scale membrane contactor experiments, two identical modules were used in which the organic phase circulates at the bore side of the modules. The effective surface area of the module with a single fiber for PSf support was

$3.5 \times 10^{-4} \text{ m}^2$  and for PP support  $3.8 \times 10^{-4} \text{ m}^2$ . The flow velocity of feed and strip phases at the shell sides were both 0.094  $\text{m s}^{-1}$ . All connecting tubes were Norprene® from Masterflex® 6404-16 (Cole-Parmer Instrument Co., USA). The total volume of the organic phase is 20 ml and the flow rate inside the tubing was 2.41  $\text{h}^{-1}$ . Both feed and strip phase volume were 200 ml. Fresh aqueous solutions were introduced before taking samples. For the large bench-scale modules, both feed and strip phases were 2 l and the organic phase is 0.170 l. All experiments were carried out at 25 °C.

### 2.4. Scanning electron microscopy

Samples for scanning electron microscopy (SEM, JEOL JSM-T220A) were made by cryogenic breaking of fibers. All samples were allowed to dry under vacuum at 30 °C overnight before coating with a thin gold layer.

## 3. Results and discussion

### 3.1. Integrity of the composite membranes

A SPEEK layer has a negligible resistance to the ion transport compared to the diffusion resistance of the impregnated liquid extraction phase inside the hydrophobic support membrane [17]. Therefore, the thickness of the top layer is not as crucial, but rather its integrity. For the fiber preparation, the concentration of a coating solution and the coating steps are of particular importance to obtain an dense coating free of macroscopic defects.

Fig. 1 shows that an increasing the number of coating times and the concentration of the coating solution result in defect free composite fibers. Less coating steps are required for the PSf support, probably due to its higher surface tension than PP and smaller pore size. A 10 wt.% SPEEK solution can readily give integral and defect free composite membranes. Thus, it is selected as the standard coating solution. Fig. 2(A) shows the cross-section of coated PSf fibers; Fig. 2(B) shows a composite membrane based on a PP support after four coating steps. Even without any hy-

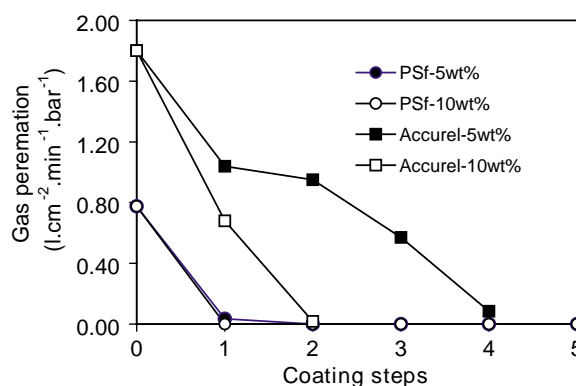


Fig. 1. Characterization of SPEEK coated composite hollow fibers by nitrogen gas permeation at room temperature. Accurel PP and PSf support membranes are coated with a 5 and 10 wt.% SPEEK solutions in methanol.

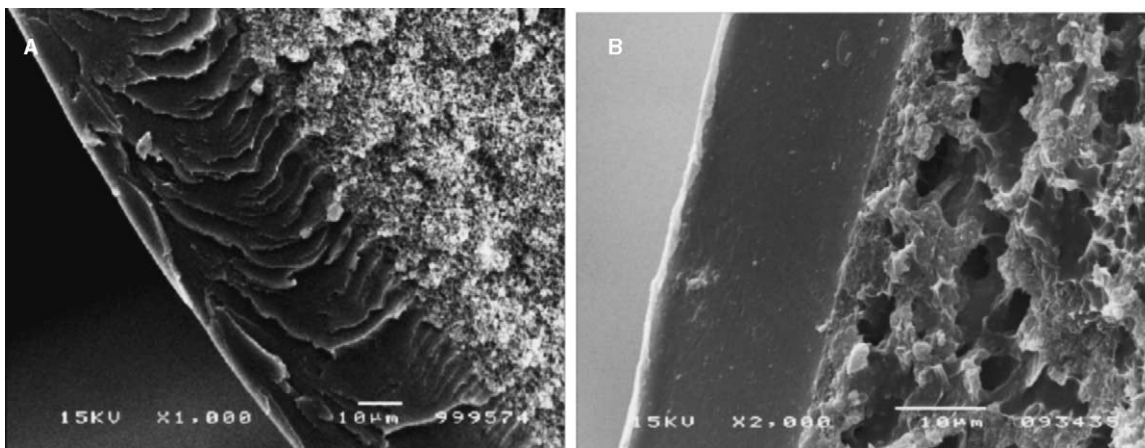


Fig. 2. SEM photos of the composite membranes with SPEEK coating layers at the shell side of the hollow fibers. (A) PSf support after two coating steps; (B) Accurel Q3/2 PP support after four coating steps. SPEEK coating solution: 10 wt.% in methanol.

drophilization pretreatment of the support membrane, adhesion between the hydrophobic support membrane and the hydrophilic stabilization layer are of sufficient quality to avoid delamination problems.

### 3.2. Copper permeation and stability in SLM

Fig. 3 shows the copper permeation of unstabilized membranes and single layer composite membranes as a function

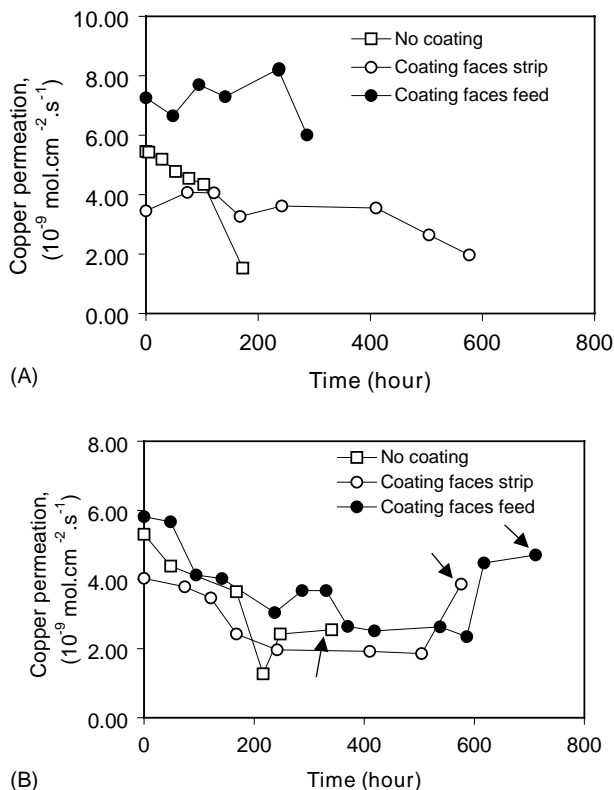


Fig. 3. Stability of hollow fiber membranes based on polysulfone (A) or Accurel Q3/2 polypropylene (B). The composite membranes face either feed or strip solutions.

of operation time in the supported liquid membrane mode. Compared to the composite membranes, the uncoated PSf and Accurel PP support membranes are rather instable indicated by a rapid drop of copper permeability in about 200 h to 25% of the original permeability. Although the composite membranes loose flux as well, we observe a fairly stable flux profile particularly at time up to 200 h. For Accurel PP support membranes, water leakage occurs as indicated by a sudden copper flux increase and the volume change of the feed and strip solutions. The results suggest that a single coating layer improves the SLM stability, however not sufficiently to stabilize system for an extended period since organic phase leaks out of the support through the uncoated side. The water leakage also indicates that loss of organic phase into the aqueous phases is the important reason of instability in the present SLM system.

Comparing the initial permeability, let us conclude that both composite membranes show higher permeability than the original membranes when the coating layer faces the feed solution. However, when the coating layer faces the strip solution, the membrane permeability declines. This phenomenon was reported before by Wijers et al. [17]: about 70% increase of copper flux was found with the feed solution at the coating side and a slight decrease with the strip solution facing the SPEEK side. Wijers et al. [17] attributed this significant increase to the pore penetration by the ion exchange layer having a lower resistance than the liquid membrane phase. In our case, since the coating layer is situated at the outside of the hollow fiber membranes, the feed flow velocity changes when altering the feed from bore to the shell side in order to have the stabilization layer facing the strip side. However, simple estimations of the mass transfer coefficients for the aqueous phases reveal that the hydrodynamic resistances are comparable for both the bore and the shell sides of the hollow fiber. Therefore, it is not a likely reason for the difference in the initial copper flux when the feed is at either the bore or shell side. When looking at the structure, we find some degree of SPEEK penetration

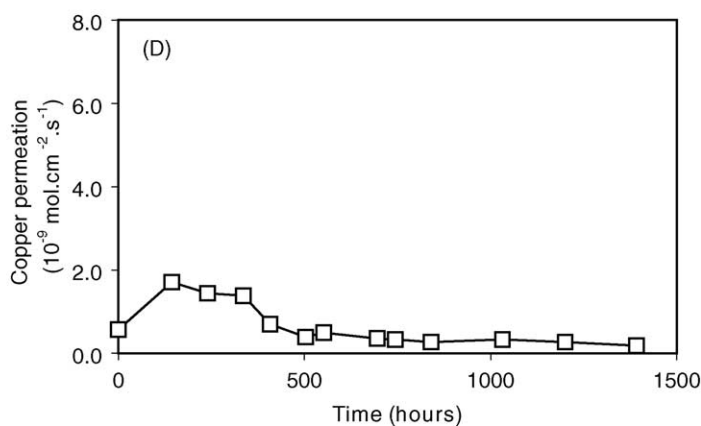
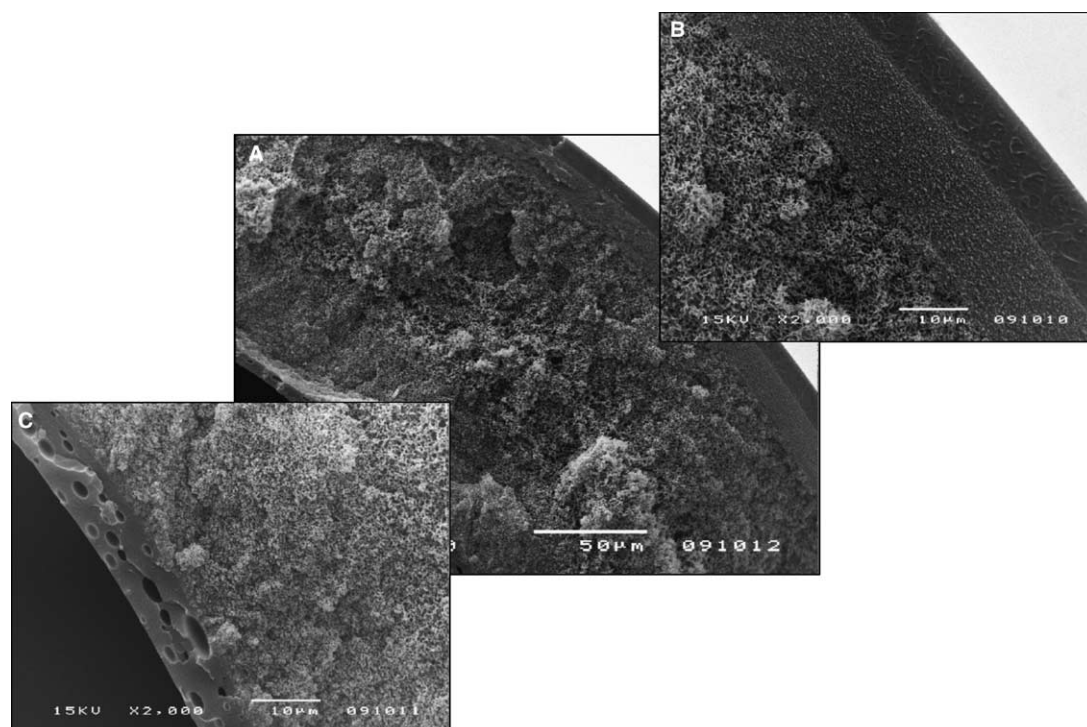


Fig. 4. SEM photos of the encapsulated composite hollow fiber membrane based on polysulfone support fiber (A)–(C) and stability of copper transport (D).

into the support membrane. Therefore, we attribute the increase in permeability (when the feed faces the stabilization layer SPEEK) to support penetration with the largest diffusional resistance in the liquid membrane extraction phase. The slight decrease in copper permeability with the strip at shell side probably stems from the low swelling of the SPEEK layer in a 2 M  $\text{H}_2\text{SO}_4$  solution. The SPEEK used (140 h sulphonation time) has rather high swelling values of in pure water (440 wt.%), 70% in a  $\text{CuSO}_4$  solution, but the least in 2 M  $\text{H}_2\text{SO}_4$  solution (48%).

### 3.3. Encapsulated hollow fiber membranes

To further improve the stability of the composite membranes, a double-layer composite membrane, or encapsu-

lated membrane, was prepared with two SPEEK layers at both the bore and shell sides and the organic phase impregnated in the support membrane in between. We carried out preliminary work and the initial results reveal two technical problems, which are related to the order of applying the second coating at the bore side and impregnating the organic phase into the support. If applying the second coating layer after the impregnation of the organic phase, a spreading problem arises due to the low surface tension characteristics of the organic phase. However, impregnating the organic phase after preparation of the double-layered composite hollow fiber membrane through the cross-sectional surface into the fiber-length direction is also problematic since the capillary forces may not be sufficient to wet the entire fiber length with extraction liquid.

Fig. 4(A)–(C) shows the structure of an encapsulated composite membrane. The coating layer at the outer surface (Fig. 4(B)) is dense and defect-free compared to the layer at the bore side (Fig. 4(C)). The later shows some macroscopic voids probably caused by the entrapped nitrogen during the evaporation step. The flux measurements as a function of time (Fig. 4(D)) show a stable but low copper permeability, which could be due to the loss of the organic phase during the preparation procedure. Considering the quality of the membranes reported by Wijers, as well as the difficulties of their preparation, these encapsulated hollow fiber membranes are significantly improved, however, require further optimization. The results must be considered a proof-of-concept: further work described below focuses on the application of single layer hollow fiber membranes in a membrane contactor configuration.

#### 3.4. Performance of composite membranes in membrane contactor

In a membrane contactor system, two modules are connected through the organic phase continuously circulating from the absorption to the desorption module and back. The organic phase circulates at the bore side of the two modules. No other process configuration was tested. Two different membrane contactor systems were tested based on two different composite PSf and Accurel PP hollow fiber membranes. Fig. 5 shows the permeability-time curves with two typical regions: a transition period and a stable operation period. The transition period is probably due to the time needed to saturate the organic phase with copper to obtain a stable copper permeation, since the membrane surface area is small compared to the large amount of organic phase. We expect shorter transition period if the membrane area is larger and the extraction liquid hold-up volume smaller.

Both systems show a stable copper flux during the experimental period. To our knowledge, this is the first data reported in literature demonstrating stable operation of a membrane contactor for liquid–liquid extraction over an ex-

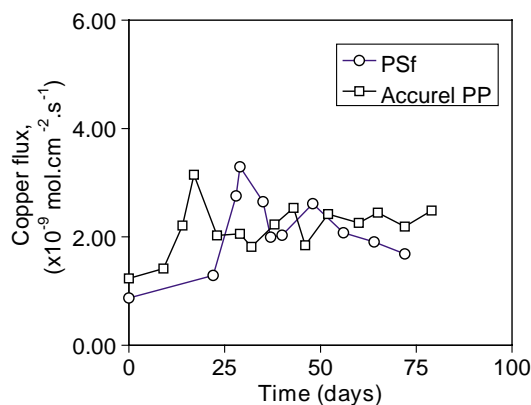


Fig. 5. Stability of PSf and Accurel PP composite hollow fiber membrane contactor.

tended period of 75 days. Averaging the last eight data points, the flux for PSf support hollow fiber-based system amounts to  $2.2 \times 10^{-9}$  and  $2.4 \times 10^{-9} \text{ mol cm}^{-2} \text{ s}^{-1}$  for Accurel PP-based system. Fig. 5 also suggests that the PP-based module operates more stable: the flux of the PSF-based system decreases to some extent. Comparison of the two operations modes, support liquid membrane mode (Fig. 3) and the membrane contactor mode (Fig. 5), leads to the conclusion that the membrane contactor mode operates more stable probably because the extraction liquid is basically encapsulated macroscopically between the composite membranes.

Now that we have developed a viable technical solution to avoid membrane instability, a further question arises with respect to the design of the membrane and scale-up of a membrane contactor system in a simple but efficient manner. In fact, to prepare and run a small bench-scale module to determine the best composite membrane for the usage in the contactor configuration, is a much too elaborate procedure. We will show for the system considered that a quick and easy experiment in the support liquid membrane configuration is an effective screening method to obtain reliable mass transport characteristics. Supposing a stable operation, there is direct relationship between the initial membrane permeability in SLM mode and the stable permeation in the membrane contactor mode. In next paragraph, a resistance-in-series model is presented and applied to support this process design strategy.

## 4. Process scale-up

### 4.1. Resistance model based on a double-layer composite membrane

To formulate a generic model describing the transport of the three liquid membrane extraction modes (SLM, encapsulated SLM and membrane contactor), our model comprises a composite hollow fiber membrane composed of two coating layers as shown in Fig. 6(A). We will show in the following derivation that the model can easily be adapted for membrane contactor mode. Also, we will demonstrate that the model applied to the SLM mode gives reliable data to model the membrane contactor mode.

Ionic transport across the membrane consists of a series of resistances, visualized as concentration profiles in Fig. 6(B). The following assumptions are used to describe the steady-state mass transfer.

1. An ion exchange coating is present at the outside and inner side of the hollow fiber with characteristic mass transport properties depending on the composition of the aqueous phase.
2. The concentration distribution at the interfaces between aqueous phase and ion exchange coating is based on Donnan exclusion. This is implicitly included in the total resistance of the coating layer.

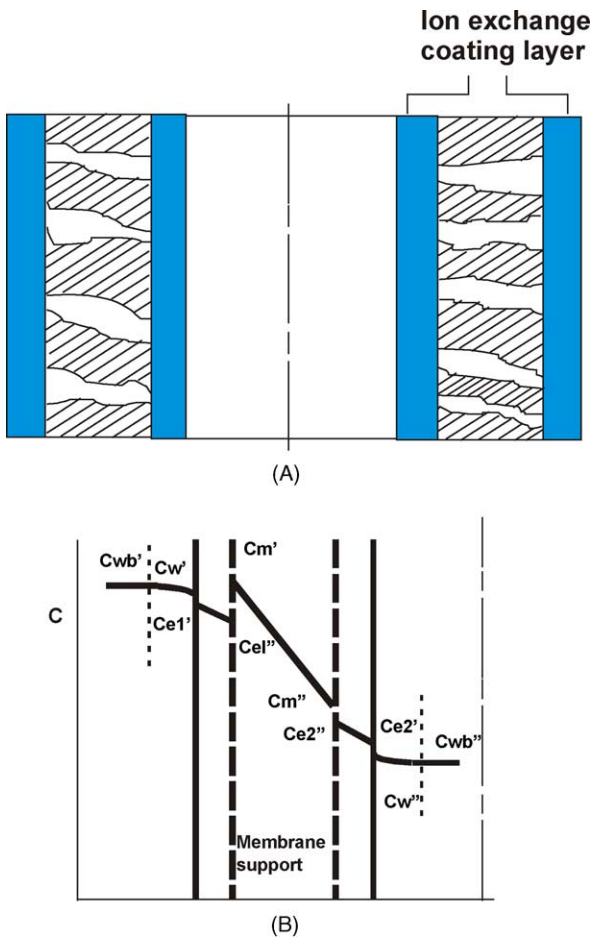


Fig. 6. Solute concentration profiles for extraction of ions with a composite hollow fiber membrane. (A) Specifications of hollow fiber; (B) concentration profiles. Dense layers refer to the hydrophilic coating.

3. Extraction reactions are rapid and can be neglected as a rate limiting step.
4. The aqueous boundary layer resistance may be combined with the membrane resistance as one-dimensional series of diffusion resistances where the hydrodynamic boundary layer resistance are negligible in comparison to the liquid membrane resistance.
5. The transport of ions through the membrane support filled with organic phase may be described by means of a membrane transfer coefficient,  $K_m$  based on the effective area of the membrane.
6. The distribution coefficient  $m$  is a constant.

A relation between the transport resistance or the overall mass transfer coefficients and all other transfer coefficient can be obtained as

$$\frac{1}{K_w d_{in}} = \frac{1}{K'_{wb} d_{out}} + \frac{1}{K_{e1} d_{e1}} + \frac{1}{m K_m d_m} + \frac{1}{K_{e2} d_{e2}} + \frac{1}{K''_{wb} d_{in}} \quad (1)$$

$K_w$  is the overall mass transfer coefficient:  $K'_{wb}$ ,  $K_m$ ,  $K''_{wb}$  are the local mass transfer coefficients for the first aqueous phase, the membrane matrix and the second aqueous phase.  $K_{e1}$  and  $K_{e2}$  are the local mass transfer coefficients for the first and the second ion exchange coating layers.  $d_{in}$ ,  $d_{out}$ ,  $d_{e1}$ ,  $d_{e2}$  and  $d_m$  represent the dimension of the hollow fiber;  $m$  is the solute distribution coefficient.

The mass transfer relationships can be obtained for a hollow fiber SLM system, either without coating or with only one coating layer using Eq. (1). For uncoated hollow fibers ( $1/K_{e1} d_{e1}$ ) and ( $1/K_{e2} d_{e2}$ ) do not exist. By assuming negligible resistances at the aqueous boundary layers (both at feed and strip side) compared to the diffusion resistance, the overall mass transfer coefficient is given as

$$\frac{1}{K_w d_{in}} \approx \frac{1}{m K_m d_m} \quad (2)$$

For a composite hollow fiber membrane with an outside coating, the total resistance to mass transfer is given as

$$\frac{1}{K_w d_{in}} \approx \frac{1}{K_{e1} d_{e1}} + \frac{1}{m K_m d_m} \quad (3)$$

For a membrane coated at the inside, Eq. (3) reads

$$\frac{1}{K_w d_{in}} \approx \frac{1}{m K_m d_m} + \frac{1}{K_{e2} d_{e2}} \quad (4)$$

Hence, we can estimate the individual mass transfer coefficients separately with negligible liquid phase boundary layer. (The flow rates for both aqueous phases and the extraction liquid are adjusted such that their laminary boundary layer thickness is small and the resistance can be neglected. This has been verified experimentally through experiments with varying liquid flow rate.)

The mass transfer in a membrane contactor configuration can be taken into account by addition of mass transfer resistance corresponding to the delivery of the organic phase from one module to the other. This can be accounted for a mass transfer coefficient  $K_o$ . For a membrane contactor consisting of two composite hollow fiber membranes, the overall mass transfer relationship can be given as

$$\frac{1}{K_w d_{in}} = \frac{1}{K_{e1} d_{e1}} + \frac{1}{m K_m d_m} + \frac{1}{K_o} + \frac{1}{m K_m d_m} + \frac{1}{K_{e2} d_{e2}} \quad (5)$$

Which includes two resistances from two coating layers ( $1/K_{e1} d_{e1}$ ) and ( $1/K_{e2} d_{e2}$ ), the porous supports ( $1/m K_m d_m$ ) and the transportation of the organic phase between the two modules ( $1/K_o$ ). If the flow rate of the organic phase is zero, a resistance close to infinity exists due to the extremely long diffusional distance between the absorber and the desorber module. However, by assuming an optimal organic phase flow rate in the lumen side of the hollow fiber, the transport resistance between two modules can be neglected, as

$$\frac{1}{K_o} \approx 0 \quad (6)$$

Table 1  
Comparison of the experimental and predicted permeation of membrane contactors based on PSf and Accurel PP Q3/2 hollow fiber membranes

Specifications			PSf	Accurel PP Q3/2
Manufacturer			Tailor-made	Membrana
Outerdiameter (mm)			0.90	1.0
Inner diameter (mm)			0.65	0.60
Pore size (nm)			52	200
Copper permeability ( $10^{-9}$ mol cm $^{-2}$ s $^{-1}$ )	SLMs [35]	Original membrane	5.1	5.3
		Coating at feed	7.2	5.8
		Coating at strip	3.4	4.0
	Contactors	Prediction	2.3	2.4
		Experimental	2.2	2.4

Coating at feed: the composite membrane with feed facing to the coating layer; coating at strip: the composite membrane with strip facing to the coating layer.

This assumption can easily be verified by comparing the transport time through the different parts. Based on residence time distribution measurements, we conclude that the contribution of tubing and pumping system is less than 10% and Eq. (6) holds for the process details described here. Thus, we have

$$\frac{1}{K_w d_{in}} = \frac{1}{K_{e1} d_{e1}} + \frac{2}{m K_m d_m} + \frac{1}{K_{e2} d_{e2}} \quad (7)$$

This equation represents the maximum transport capacity of a contactor system with two hollow fiber modules. The model needs only three small scale experiments for the parameter evaluation, i.e. a transport of a fiber without coating (Eq. (2)), transport of a fiber with a coating facing the feed phase (using Eq. (3)) and with the coating layer at the strip side (using Eq. (4), notice the coating is at outside surface).

#### 4.2. Results

Table 1 shows the properties of the support membranes and the experimentally determined copper fluxes before and after coating with the stabilization layer in the SLM mode. These values are used for the above described model for the membrane contactor mode. The predicted and experimental results for the contactor mode are compared as well in Table 1. For the comparison, the predicted values for both PSf and PP membranes compare well with the experimental values. It indicates the feasibility of the resistance model in the description of the transport process of a membrane contactor. We conclude that a higher ion flux in the contactor mode can be obtained by decreasing the diffusion transport resistance in the support membrane. Ideally, one desires to have a ion exchange hollow fiber at hand without any porous support.

## 5. Conclusions

Ion exchange material coated composite hollow fiber membranes were prepared for solving the instability problems in liquid membrane extraction. Significant stability

improvement was found in SLM application. Very stable operation in membrane contactor application was demonstrated for a continuous operation of about 75 days. Moreover, a large bench-scale membrane contactor was carried out with two modules of surface area of 0.064 m $^2$ . A model to predict the permeability of membrane contactor was developed and found to be sufficiently accurate. First proof-of-principle of encapsulated composite membrane showed promising results. We propose a stable membrane contactor system composed of hollow fiber ion exchange membranes without any support membrane to be a viable solution to the large-scale application.

### Nomenclature

$C'_{e1}, C''_{e1}$	ion concentration in the first ion exchange coating at aqueous and organic sides (mol L $^{-3}$ )
$C'_{e2}, C''_{e2}$	ion concentration in the second ion exchange coating at aqueous and organic sides (mol L $^{-3}$ )
$C'_m, C''_m$	concentration of ion-organic complex in the organic phase at two coating layers and organic interfaces, respectively (mol L $^{-3}$ )
$C'_w, C''_w$	ion concentration at two interfaces between aqueous and coating layers (mol L $^{-3}$ )
$C'_{wb}, C''_{wb}$	ion concentration in two bulk aqueous phases (mol L $^{-3}$ )
$d_e$	hydraulic diameter for shell side (L) (four cross-section area/wetted perimeter)
$d_{e1}$	effective diameter of the first coating layer (L)
$d_{e2}$	effective diameter of the second coating layer (L)
$d_i$	inner diameter of the hollow fiber (L)
$d_{in}$	inner diameter of the composite fiber membrane (L)
$d_m$	effective diameter of the liquid membrane layer (L)



$d_o$	outer diameter of the hollow fiber (L)
$d_{out}$	Outer diameter of the composite fiber membrane (L)
$d_s$	inner diameter of module for shell side (L)
$D_{AB}$	solute diffusivity ( $L^2T^{-1}$ )
$k$	local mass transfer coefficient in the aqueous phase ( $LT^{-1}$ )
$K_{e1}$	mass transfer coefficient when coating at the shell side ( $LT^{-1}$ )
$K_{e2}$	mass transfer coefficient when coating at the bore side ( $LT^{-1}$ )
$K_m$	membrane mass transfer coefficient for ions ( $LT^{-1}$ )
$K_o$	mass transfer coefficient from transport of the organic phase from feed module to strip module ( $LT^{-1}$ )
$K_w$	overall mass transfer coefficient based on aqueous phase ( $LT^{-1}$ )
$K'_{wb}$	local mass transfer coefficient in the first aqueous phase ( $LT^{-1}$ )
$K''_{wb}$	local mass transfer coefficient in the second aqueous phase ( $LT^{-1}$ )
$l$	length of the hollow fiber (L)
$m$	solute distribution coefficient: ratio of organic phase solution concentration to aqueous phase solute or solution concentration in ion exchange materials
$Sc$	Schmidt number
$Sh$	Sherwood number
<i>Greek letters</i>	
$\delta$	boundary layer thickness (L)
$\gamma$	surface tension ( $LT^{-2}$ )
$\mu$	viscosity ( $ML^{-1}T^{-1}$ )
$\rho$	liquid density ( $ML^{-3}$ )
$\varpi$	liquid flow rate ( $LT^{-1}$ )

## References

- [1] A.J.B. Kemperman, D. Bargeman, T. van den Boomgaard, H. Strathmann, Stability of supported liquid membranes: state of the art, *Sep. Sci. Technol.* 31 (1996) 2733–2762.
- [2] A.M. Neplenbroek, D. Bargeman, C.A. Smolders, Supported liquid membranes: stabilization by gelation, *J. Membr. Sci.* 67 (1992) 149–165.
- [3] L. Bromberg, G. Levin, O. Kedem, Transport of metals through gelled supported liquid membranes containing carrier, *J. Membr. Sci.* 71 (1992) 41–50.
- [4] G. Levin, L. Bromberg, Gelled membrane composed of diocetylthiocarbamate substituted on poly(vinylchloride) and di(2-ethylhexyl) dithiophosphoric acid, *J. Appl. Polym. Sci.* 48 (1993) 335–341.
- [5] A.M. Neplenbroek, Stability of supported liquid membranes, Ph.D. thesis, University of Twente, Enschede, 1989.
- [6] A.J.B. Kemperman, B. Damink, T. van den Boomgaard, H. Strathmann, Stabilization of supported liquid membranes by gelation with PVC, *J. Appl. Polym. Sci.* (1997) 1205–1215.
- [7] C. Wijers, Supported liquid membranes for removal of heavy metals: permeability, selectivity and stability, Ph.D. thesis, University of Twente, Enschede, 1996.
- [8] C. Clement, M.M. Hossain, Stability of a supported liquid membrane for removing hydrophobic solutes from casein hydrolysate solution, *Sep. Sci. Technol.* 32 (1997) 2685–2703.
- [9] A.J.B. Kemperman, H.H.M. Rolevink, T. van den Boomgaard, H. Strathmann, Stabilization of supported liquid membranes by interfacial polymerization top layers, *J. Membr. Sci.* 138 (1998) 43–55.
- [10] M.C. Wijers, M. Wessling, H. Strathmann, Limitation of the lifetime stabilization of supported liquid membrane by polyamides layers, *Sep. Purif. Technol.* 17 (1999) 147–157.
- [11] Y. Wang, Y.S. Thio, F.M. Doyle, Formation of semi-permeable polyamide skin layers on the surface of supported liquid membranes, *J. Membr. Sci.* 147 (1998) 109–116.
- [12] X.J. Yang, A.G. Fane, J. Bi, H.J. Griesser, Stabilization of supported liquid membranes by plasma polymerization surface coating, *J. Membr. Sci.* 168 (2000) 29–37.
- [13] O. Kedem, L. Bromberg, Ion-exchange membranes in extraction processes, *J. Membr. Sci.* 78 (1993) 255–264.
- [14] V.S. Kislik, A.M. Eyal, Hybrid liquid membrane (HLM) and supported liquid membrane (SLM) based transport of titanium, *J. Membr. Sci.* 111 (1996) 271–281.
- [15] V.S. Kislik, A.M. Eyal, Hybrid liquid membrane (HLM) system in separation technologies, *J. Membr. Sci.* 111 (1996) 259–272.
- [16] R. Wodzki, G. Sionkowski, Recovery and concentration of metal ions. II. Multimembrane hybrid system, *Sep. Sci. Technol.* 30 (1995) 2763–2778.
- [17] M.C. Wijers, M. Jin, M. Wessling, H. Strathmann, Supported liquid membranes modification with sulphonated poly(ether ether ketone): permeability, *J. Membr. Sci.* 147 (1998) 117–130.
- [18] K. Sirkar, B.W. Reed, EP0771585 (1997).
- [19] K. Sirkar, US5053132 (1991).
- [20] W.S. Ho, T.K. Poddar, New membrane technology for removal and recovery of chromium from waste waters, *Environ. Prog.* 20 (2001) 44–52.
- [21] W.S. Ho, T.K. Poddar, New membrane technology for removal and recovery of metals from waste waters and process streams, in: *Proceedings of the AIChE Spring National Meeting*, Atlanta, GA, 2000, pp. 38–43.
- [22] W. Ho, T. Poddar, B. Wang, Removal and recovery of metals by supported liquid membranes with strip dispersion, in: *Proceedings of the 12th Annual Meeting North American Membrane Society*, Lexington, KY, USA, 2001.
- [23] B.W. Reed, M.J. Semmens, E. Cussler, Membrane contactors, in: R.D. Noble, S.A. Stern (Eds.), *Membrane Separations Technology. Principles and Applications*, Elsevier, Amsterdam, 1995, pp. 467–498.
- [24] K. Sirkar, Membrane separation technologies: current developments, *Chem. Eng. Commun.* 157 (1997) 145–184.
- [25] A. Gabelman, S.T. Hwang, Hollow fiber membrane contactors, *J. Membr. Sci.* 159 (1999) 61–106.
- [26] A. Sengupta, R. Basu, R. Prasad, K.K. Sirkar, Separation of liquid solutions by contained liquid membranes, *Sep. Sci. Technol.* 23 (1988) 1735–1751.
- [27] A.K. Guha, C.H. Yun, R. Basu, K. Sirkar, Heavy metal removal and recovery by contained liquid membrane permeator, *AIChE J.* 40 (1994) 1223–1237.
- [28] D.K. Mandal, A.K. Guha, K.K. Sirkar, Isomer separation by a hollow fiber contained liquid membrane permeator, *J. Membr. Sci.* 144 (1998) 13–24.
- [29] R. Basu, K.K. Sirkar, Hollow fiber contained liquid membrane of citric acid, *AIChE J.* 37 (1991) 383–393.
- [30] M. Teramoto, N. Tohno, N. Ohnishi, H. Matsuyama, Development of a spiral-type flowing liquid membrane module with high stability

- and its application to the recovery of chromium and zinc, *Sep. Sci. Technol.* 24 (1989) 981–999.
- [31] M. Teramoto, H. Matsuyama, T. Yonehara, Selective facilitated transport of benzene across supported and flowing liquid membranes containing silver nitrate as carrier, *J. Membr. Sci.* 50 (1990) 269–284.
- [32] M. Teramoto, H. Matsuyama, T. Yamashiro, S. Okamoto, Separation of ethylene from ethane by a flowing liquid membrane using silver nitrate as a carrier, *J. Membr. Sci.* 45 (1989) 115–136.
- [33] S. Schlosser, I. Rothova, A new type of hollow-fiber pertractor, *Sep. Sci. Technol.* 29 (1994) 765–780.
- [34] I.M. Coelho, P. Silvestre, R.M.C. Viegas, J.P.S.G. Crespo, M.J.T. Carrondo, Membrane-based solvent extraction and stripping of lactate in hollow-fiber contactors, *J. Membr. Sci.* 134 (1997) 19–32.
- [35] R. Prasad, K.K. Sirkar, Membrane-based solvent extraction, in: W.S.W. Ho, K.K. Sirkar (Eds.), *Membrane Handbook*, Van Nostrand Reinhold, New York, 1992.